Interaction Notes

Note 632

12 November 2019

Transformer Responses to Fast Transient Excitations

and
Mr. Markus Nyffeler
armasuisse, Switzerland

Abstract

This note documents a literature search on the effects of fast electrical transients on power system transformers, for the purpose of estimating the effects of a high-altitude electromagnetic pulse (HEMP) on transformers. In this study, data for both the HEMP signal attenuation and distortion as it propagates through the transformer, and for possible damage to the transformer has been found, and the measurement programs that developed these results are discussed. Unfortunately, only a limited number of results have been found, so the generalization of these measurements to a wide variety of different transformers is difficult. However, these results do provide some insight into transformer operation in an HEMP environment.

.

1. Introduction

A previous study of high-altitude electromagnetic pulse (HEMP) effects on electrical power systems has concluded that power transformers can play an important role in determining the nature of the electrical surges that may be conducted into a facility [1]. While this report treated only the loading of the power distribution line by the transformer, there is evidence that the transformer will modify the HEMP surge that propagates through this circuit element, thereby modifying the response of load equipment.

For a facility or equipment that is subjected to an HEMP event, there are important issues that need to be addressed in relation to the power system excitation. The first is the understanding of how a fast transient surge induced on a power line will be modified by the transformer. If such a surge is not highly attenuated by the transformer, it may cause damage to more sensitive components within the system. The second issue is to understand if the transformer itself can be damaged by the surge.

To understand these two issues, it is useful to examine and summarize existing data on the responses of power transformers to fast electrical surges. Over the past ten to fifteen years, some work on fast-pulse responses of transformers has been undertaken, but unfortunately, much of this work has not been reported in the literature, or it has been poorly documented. This note serves to review the some of the available data and literature in this area, and to summarize what has been found about transformer responses to transient excitations.

2. High Frequency Models for Power Transformers

Within the power community, a transformer is thought of as low-frequency power system component, which operates in the 50 to 60 Hz frequency range. An often-used model for a transformer at these frequencies consists of two magnetically coupled coils, as shown in Figure 1. Other more complicated models can be envisioned that will take into account the fringing of the magnetic flux within the coils, the resistive losses in the transformer windings and magnetic core, and the core magnetization.

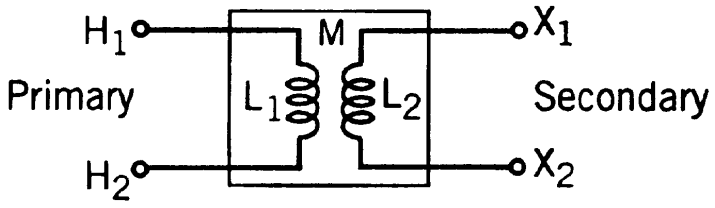

Figure 1. A low-frequency transformer model.

The testing of transformers at higher frequencies shows that the simple transformer model in Figure 1 is inadequate, primarily due to the effects of the parasitic circuit elements. Vance [2] has suggested a possible high-frequency model for a transformer, and this is shown in Figure 2. While such a model is useful for understanding high-frequency transformer operation, it is not useful for HEMP calculations involving transformers, because the numerical values for the circuit parameters are unknown.

Frequently, the best source of information for the parasitic element values for a particular transformer will be the manufacturer, who has knowledge of the construction details of the device, and may have measured or calculated some of them. However, these data may be proprietary to the manufacturer, and they may not be freely available. As a consequence of this lack of data, other types of transformer measurements can be performed. The results of some of these measurements will be discussed in this note.

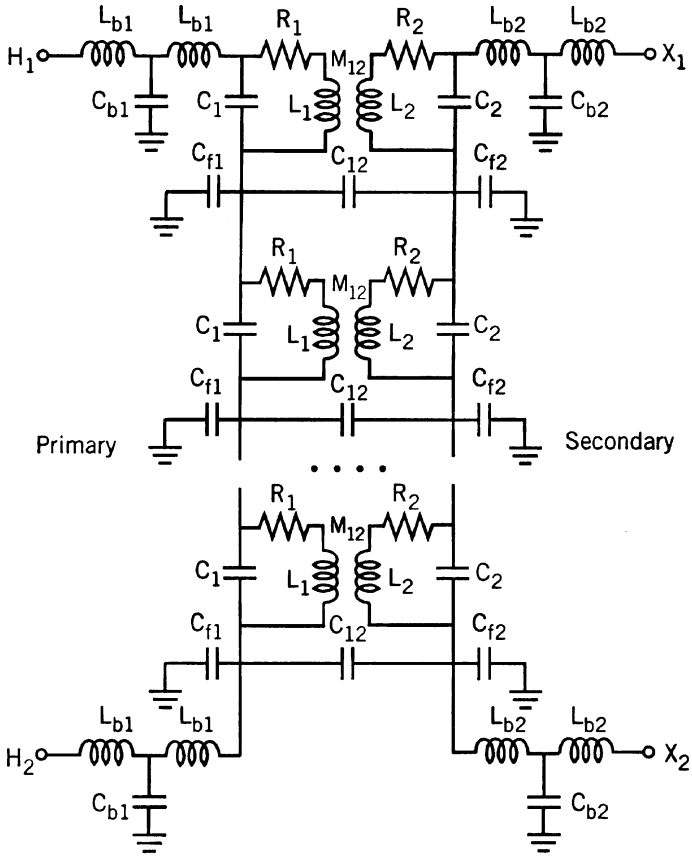

Primary

L_1 = self inductance of winding
C_1 = turn-to-turn capacitance
R_1 = winding resistance
L_{b1} = bushing inductance
C_{b1} = bushing capacitance
C_{f1} = winding-case capacitance

Secondary

L_2 = self inductance of winding
C_2 = turn-to-turn capacitance
R_2 = winding resistance
L_{b2} = bushing inductance
C_{b2} = bushing capacitance
C_{f2} = winding-case capacitance

Mutual

M_{12} = mutual inductance between primary and secondary
C_{12} = coupling capacitance between primary and secondary

Figure 2. A high-frequency transformer model (from [2]).

3. Transformer Response Testing

In examining the literature relating to fast-pulse transformer responses, several test programs have been found that provide insight into the signal degradation in transformers. Typically, attention is paid to how the transformer attenuates the peak amplitude of the HEMP surges passing through it. This attenuation can be characterized by either a voltage transfer function V_{out}/V_{in} or a current transfer function I_{out}/I_{in}.

It is common that transformer testing is performed under loaded conditions, with either the transformer conducted to the power system, or with a load impedance that simulates the power line impedances. Some of the transformers that were tested had surge protection devices placed on the input or output (i.e., primary or secondary) circuits, and these can change the effective surge attenuation by changing both the impedance levels and the spectral content of the pulses.

The following sections describe various transformer attenuation tests and their results.

3.1. Pulse measurements on a Swedish power generation plant

In 1984 a pulse injection test was performed at an oil-burning power generation plant in Vasteraas, Sweden [3]. In this test, the power generation station was disconnected from the power grid at the entry point to the facility. At this location, a low-level pulse generator designed by the Swedish Defense Research Institute was attached to one of the three 70 kV phase conductors. As shown Figure 3, several different observation points within the power plant were identified for the purpose of investigating the behavior of the injected transient signal as it propagated through the system.

Based on extrapolations of the low level experimental data of ref.[3], the internal responses for an external HEMP field exciting an external power transmission line connected to the generation station were determined [4]. For this calculation, it was assumed that a 20 m high-power transmission line was excited by a 25 kV/m incident field striking the line with near grazing incidence. The earth conductivity was assumed to be σ = 0.1 S/m.

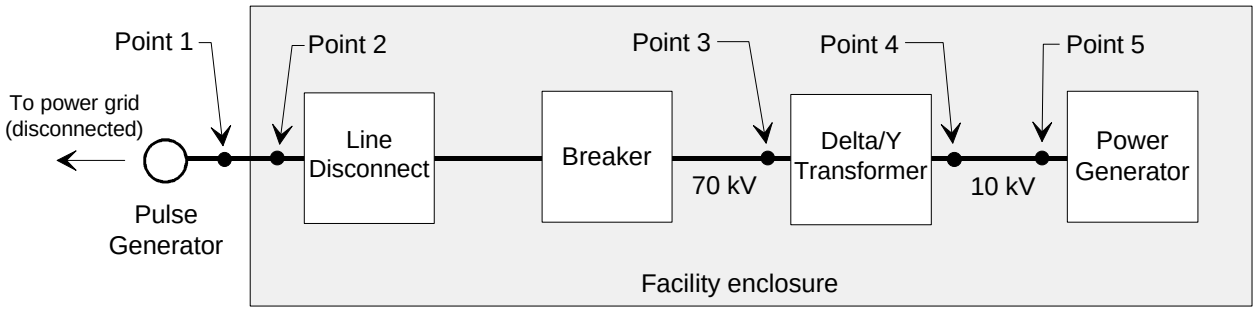

Figure 3. Illustration of the pulse injection test configuration of the Swedish power generation facility.

As the measurements in [3] were the phase conductor currents, the extrapolated results of ref.[4] provided the HEMP-induced phase currents. Table 1 presents a summary of the extrapolated peak HEMP-induced currents within this Swedish power generation facility. It is interesting to note that the attenuation of the HEMP current surge through the transformer (between location 3 and 4 in the figure) is approximately 14 dB.

Table 1. Summary of the extrapolated peak HEMP-induced currents within the power generation facility (from [4]).

Location	Peak Current (kA)	Attenuation (dB)
1	7.0	0.0
2	3.0	7.3
3	2.0	11.0
4	0.4	25.0
5	0.25	29.0

3.2. 25 kVA transformer & filter tests

In 1989, Maxwell Laboratories performed a current injection test on a 4160V/120V 25-kVA distribution transformer [5]. The transformer under test is shown in Figure 4, and the experimental set-up included various protection devices, including nonlinear surge arresters on the primary circuit, a transorb protector on the output, as well as a passive filter at the load.

The reported goal of this test was to simulate HEMP effects of a realistic service entrance of a power distribution system, and to determine the effects of the various power system protection elements on the induced surges. To simulate the HEMP surge on the line, a radiating EMP simulator consisting of a 2.2 – 2.5 MV Marx generator and a 60 Ω monocone antenna was connected to a 15 kV XLPE 2 AWG power cable through a 200 Ω resistance simulating the surge impedance of an overhead power distribution line. This modified pulser provided an injected current and voltage onto the power system and eventually into the transformer.

The 15 kV power cable was located within a 6.35 cm OD rigid conduit (denoted as the “shield” in the figure) in an attempt to simulate the effects of a transition from an overhead line to a "terminator” or “pothead” in the power system. On the source side of this cable, a surge arrestor was installed, and another surge arrestor was located at the input terminals of the transformer.

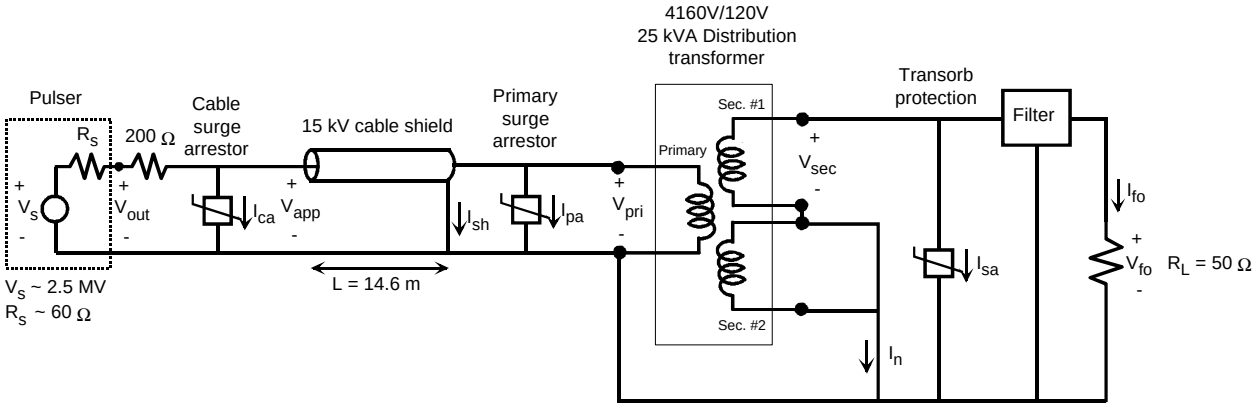

Figure 4. Configuration and circuit diagram for the 25 kVA transformer and filter test.

The transformer had two secondary circuits. One was connected to a 50 Ω load impedance through the transorb and a commercial power filter. The other secondary circuit was short-circuited and connected to the neutral. Unfortunately, in the final test report, no details were provided regarding the nature of the filter or the nonlinear protection devices.

The Marx generator reportedly produced a voltage waveform having a rise-time (zero to peak) of about 20 ns and a decay time (to 1/e of peak) of about 1 μs. The amplitude was variable, with the loaded pulser output voltage V_{out} ranging from about 1 to 2 MV. With this variable source, a series of measurements was made for the simulated power system in the following configurations:

- Configuration #1 – Power system as illustrated in Figure 4 with all protection installed
- Configuration #2 – Power system as in #1, but without transorb protection on the secondary circuit
- Configuration #3 – Power system as in #2, but without surge protection in the primary circuit
- Configuration #4 – Power system as in #2, but without the cable surge arrestor
- Configuration #5 – Power system with all nonlinear protection removed, but with the filter still installed

Unfortunately, the HEMP-induced currents flowing on the incoming power line and on the transformer connections were not measured. The only currents measured were on the cable shield to ground connection, the transformer neutral connection, the surge arresters and transorb, and the 50 Ω load. More useful in describing the behavior of this system to HEMP excitation are the measured voltages. These were the applied voltage at the input of the 15 kV cable, V_{app}, the voltage induced across the primary of the transformer, V_{pri}, the transformer secondary voltage, V_{sec}, and the load voltage, V_{fo}. These voltages serve to illustrate the degree of attenuation that the HEMP surge experiences as it propagates through the system.

Figure 5 summarizes the measured voltage responses in this test, showing the various peak voltages as a function of the pulser output voltage V_{out} for the five different system configurations. These data are presented as ratios of the measured voltage, divided by the pulser output voltage. For configurations #1 through #3, the pulser voltage was changed over a range of values, and this permits the development of a response plot versus the output voltage. For configurations #4 and #5, however, the measurements reported in [5] were only for a pulser voltage of about 1 MV. Consequently, for these latter cases, only single data points exist.

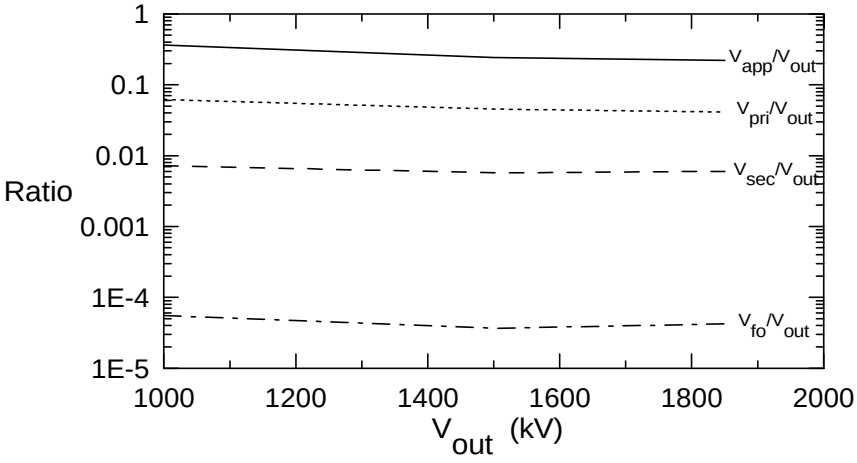

a. Responses for configuration #1

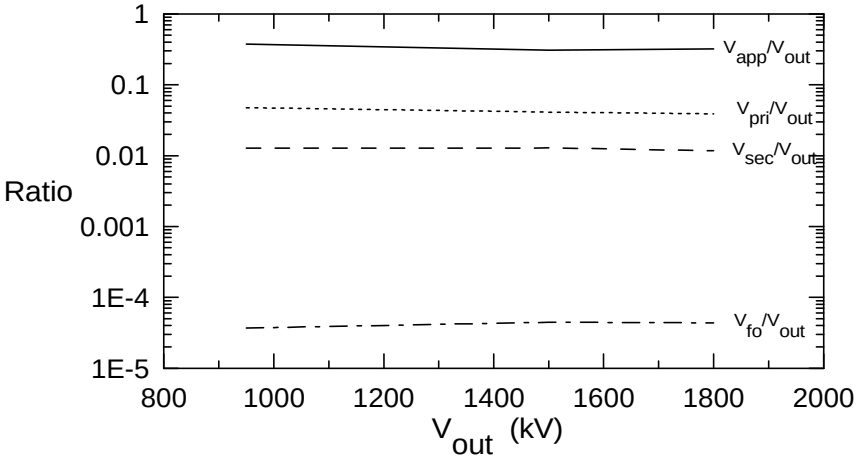

b. Responses for configuration #2

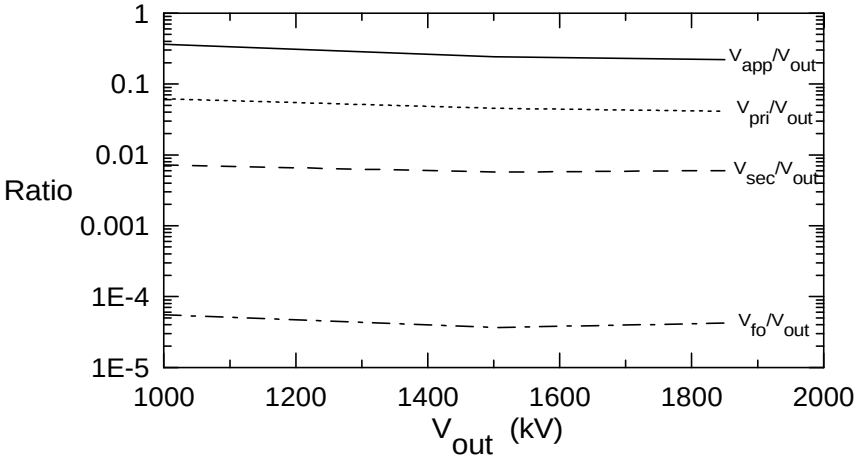

c. Responses for configuration #3

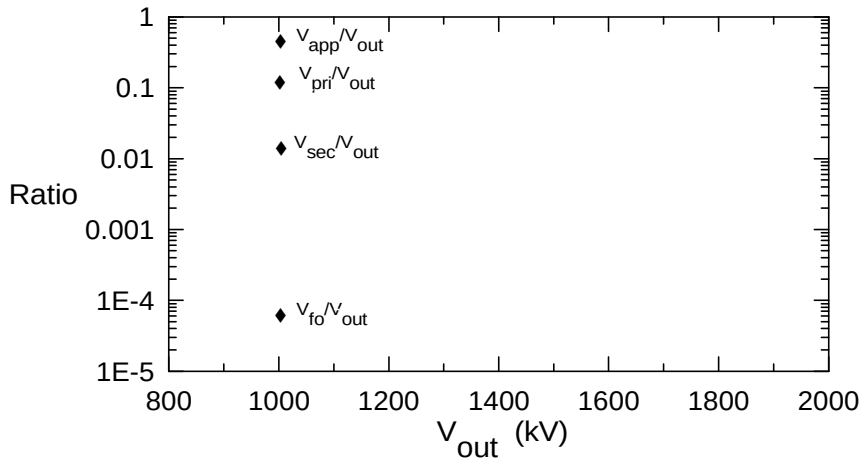

d. Responses for configuration #4

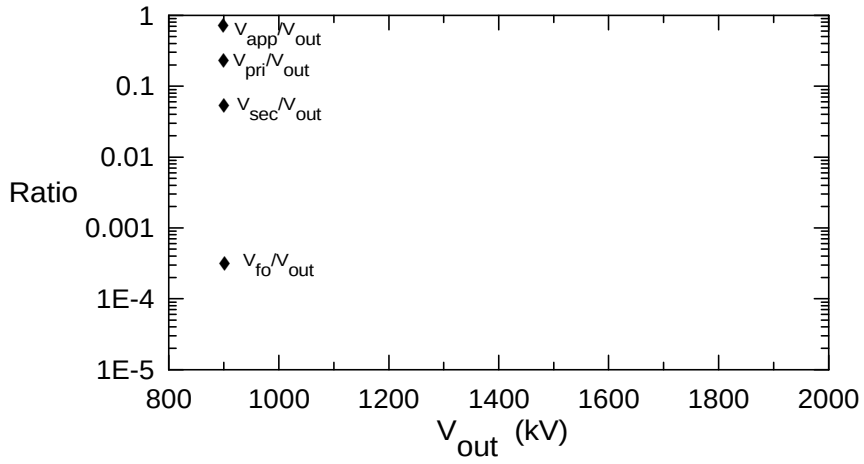

e. Responses for configuration #5

Figure 5. Plots of the measured peak voltages for different pulser output voltages V_{out}.

The data in Figure 5 can be summarized by noting that there is a very slow change of the responses with the pulser voltage. By averaging the voltage attenuation ratios for each configuration, the data presented in Table 2 may be developed. In this table we note that the final load voltage response V_{fo} is largely insensitive to the protection measures that appear at the source side of the test setup. This is probably due to the fact that the load filter (which was never removed during the test) provides a good degree of protection.

The data in this table illustrate that configuration #1 has the best protection, with configuration #5 having the least protection. The attenuation of the HEMP surge by the transformer can be estimated by taking the average of the differences of V_{pri}/V_{out} and V_{sec}/V_{out}. From the data presented here, we see that the transformer provides a voltage attenuation of roughly 14.4 dB, which is comparable with the attenuation of the current estimated in Section 3.1 for the Swedish measurements.

Table 2. Averaged voltage attenuation ratios for the transformer/filter system.

System Configuration	V_{app}/V_{out} (dB)	V_{pri}/V_{out} (dB)	V_{sec}/V_{out} (dB)	V_{fo}/V_{out} (dB)
1	-11.2	-26.2	-44.0	-87.0
2	-9.5	-27.5	-38.1	-87.6
3	-9.1	-21.5	-36.3	-84.2
4	-4.7	-19.2	-35.9	-85.2
5	-1.7	-11.8	-24.0	-70.2

While the induced voltages within the transformer and other system components were substantial in this test, and other tests have confirmed component damage or failure, there was nothing mentioned in this report of damage occurring within the transformer.

3.3. Silicon steel and amorphous core transformer tests.

Maxwell Laboratories also performed HEMP surge tests on three 25 kVA silicon steel and three amorphous core transformers in 1989. The stated purpose of these tests was to compare the HEMP vulnerability of transformers made with silicon steel core to those constructed with amorphous steel cores. Results from this test program are documented in [6].

For these tests, the same power system mockup used for the transformer/filter tests discussed in Section 3.2 was used. However, the electrical loads at the 110 V secondary of the transformer were balanced, with two 50 Ω loads being placed across each winding. In addition, the secondary circuit filter and transorb was removed, resulting in the circuit diagram shown in Figure 6.

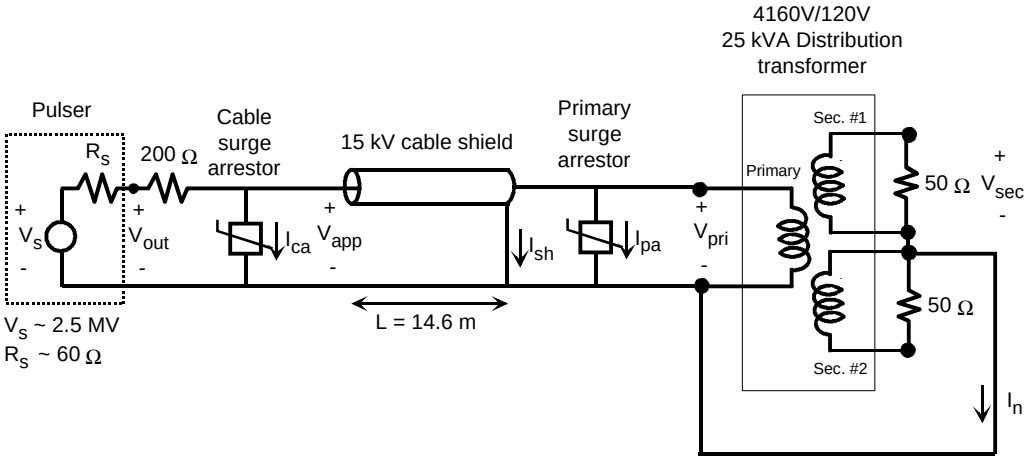

Figure 6. Configuration and circuit diagram for the silicon steel and amorphous core 25 kVA transformer tests.

For these tests, two different system configurations were considered:

- Configuration #1 – Power system as illustrated in Figure 6 with all protection installed
- Configuration #2 – Power system as illustrated in Figure 6 with all protective measures removed

The results of these tests are summarized in Figure 7 for the silicon steel transformers, and in Figure 8 for the amorphous core transformers. In these figures, the ratios of the measured voltages V_{app}/V_{out}, V_{pri}/V_{out} and V_{sec}/V_{out} are plotted as a function of the pulser output voltage V_{out}. Note that the configuration #1 data are presented in the form of curves, while the configuration #2 data, which had been taken for only one value of the output voltage, are shown by the isolated data points.

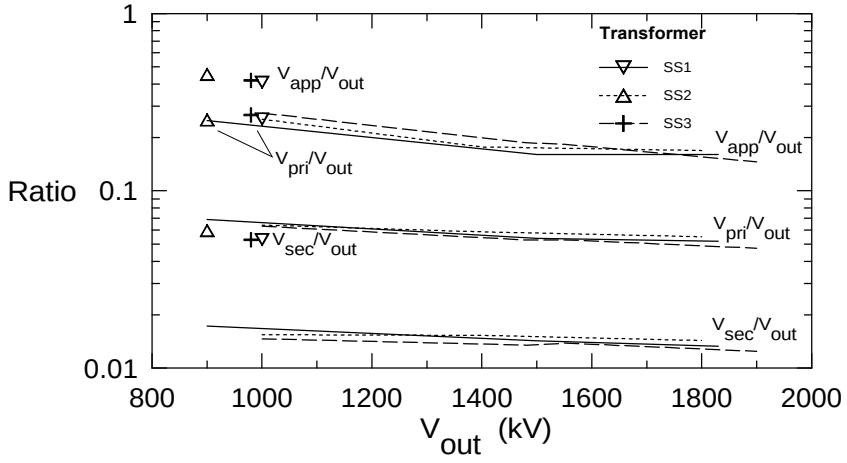

Figure 7. Plots of the measured peak voltages for the three silicon steel core transformers. (Configuration #1 data are the curves, and configuration #2 data are the isolated points.)

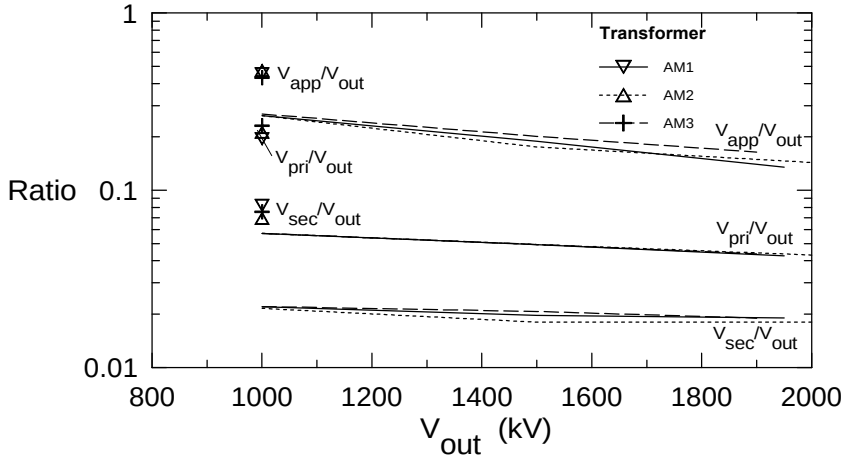

Figure 8. Plots of the measured peak voltages for the three amorphous steel core transformers. (Configuration #1 data are the curves, and configuration #2 data are the isolated points.)

As in the previous transformer/filter test in Section 3.2, the voltage response ratios are reasonably constant, and thus may be averaged to provide a single number representing the attenuation of the HEMP surge within the transformer. Table 3 summarizes the averaged voltage attenuation ratios for the silicon and amorphous core transformers for both configurations. From these data it is apparent that the silicon steel core transformer provides a surge attenuation that is slightly better than that of the amorphous core transformer. For the protected configuration of the power system (configuration #1), the transformers provide an average shielding factor of 12.6 dB, which is roughly comparable to the 14.4 dB attenuation found from the previous test.

For configuration #2 with the protection elements removed, the voltage attenuation due to the transformer is slightly lower at 11.2 dB. This difference is possibly due to the change in the wave shapes in the protected and non-protected cases.

Table 3. Averaged voltage attenuation ratios for the 25 kVA silicon steel and amorphous core transformer systems.

System Configuration	V_{app}/V_{out} (dB)	V_{pri}/V_{out} (dB)	V_{sec}/V_{out} (dB)
Silicon Steel Core (Config.#1)	-14.2	-24.9	-36.8
Amorphous Core (Config.#1)	-14.0	-26.0	-34.1
Silicon Steel Core (Config.#2)	-7.4	-11.8	-25.2
Amorphous Core (Config.#2)	-6.9	-13.4	-22.4

3.4. CW and pulse testing of a 1.2 kV distribution transformer

The previously discussed transformer characterization measurements have been made with the transformer located within the power system – connected to a particular input and output circuit. Consequently, such measurements characterize the transformer only in that specific installation, and it is difficult to be able to accurately infer how the transfer might perform if it were at another facility.

To eliminate this problem, a measurement program to characterize the wideband electrical properties of an Allis-Chambers 1.2 kV-120/240 V distribution-class transformer was conducted. As discussed in ref. [7], such a power transformer can be represented by a general four-port network shown in Figure 9a. For this transformer, broadband CW measurements of the scattering (S) parameters for the transformer were made, both in magnitude and phase. This results in a 4×4 frequency-dependent, complex-valued matrix that describes the transformer port responses using the representation of Figure 9b.

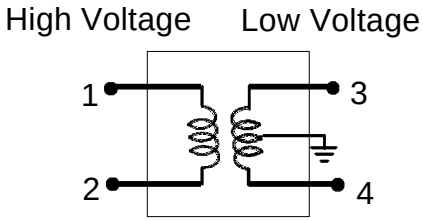

(a) Low-frequency model of the physical transformer

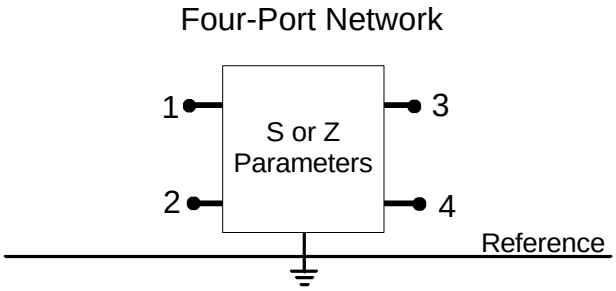

(b) Four-port representation of the transformer

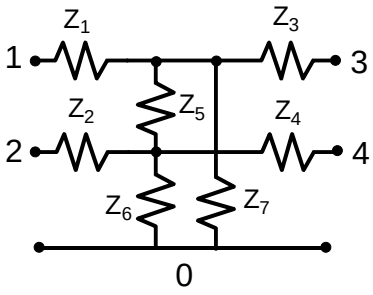

(c) Lumped element Tee-equivalent circuit for the transformer

Figure 9. Representation of the 1.2 kV-120/240 V distribution transformer.

One possible lumped circuit realization of this transformer is shown in Figure 9c, which is the equivalent Tee circuit. As in the case of simpler two-ports, there is no guarantee that the various impedance elements be physically realizable (i.e., containing positive real (PR) impedances). Using the measured s-parameters, the short-circuit impedance parameters z_{ij} can be derived using the standard transformations given in ref. [8]. From these z-parameters, the values of the impedance circuit elements Z_i in Figure 9c can be found.

Assuming that the transformer is symmetric in its windings leads to the conclusion that $Z_1 = Z_2$, $Z_3 = Z_4$, and $Z_6 = Z_7$. Figure 10 presents the frequency dependent impedances representing the transformer. Notice that at low frequencies, the impedance elements on the transformer primary (Z_1 and Z_2) illustrate a capacitive reactance with a positive real part, which can be represented by a resistance. Such a capacitive reactance is not noted for the secondary circuit in Figure 10b.

The resistance components of the elements Z_1, Z_2, Z_3 and Z_4 are positive for all frequencies, indicating that these elements can be represented by physical resistances, together with some combination of reactive elements to account for the resonances. Elements Z_6 and Z_7 in Figure 10c exhibits a negative resistance for some frequencies, and this implies that this element is not physically realizable. However, this does not detract from the ability of this circuit in *mathematically* representing the behavior of the transformer at its terminals.

Element Z_5, which is the impedance element between the two ports of the transformer, is shown in Figure 10d. Notice that this impedance is significantly lower than the other impedances in the Tee network. As a consequence, it appears to be more affected by the noise in the measurements and in the numerical reconstruction of the element values.

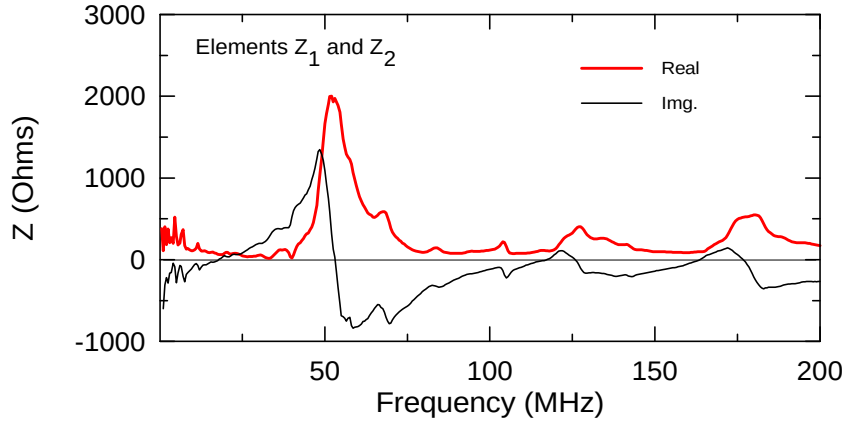

a. Elements Z_1 and Z_2

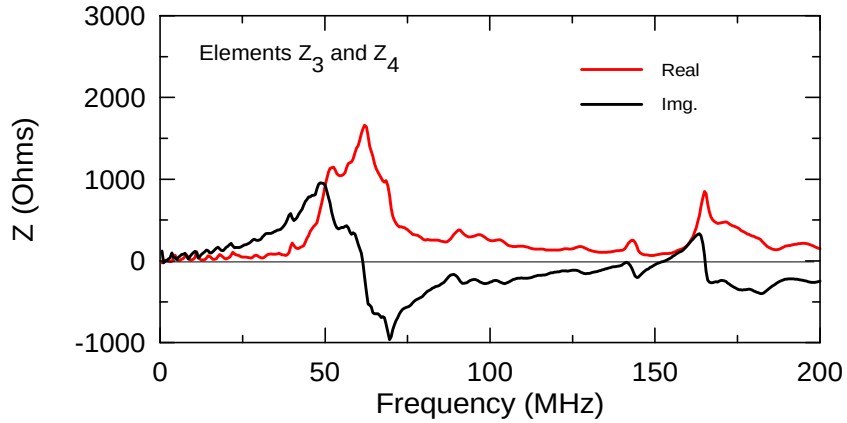

b. Elements Z_3 and Z_4

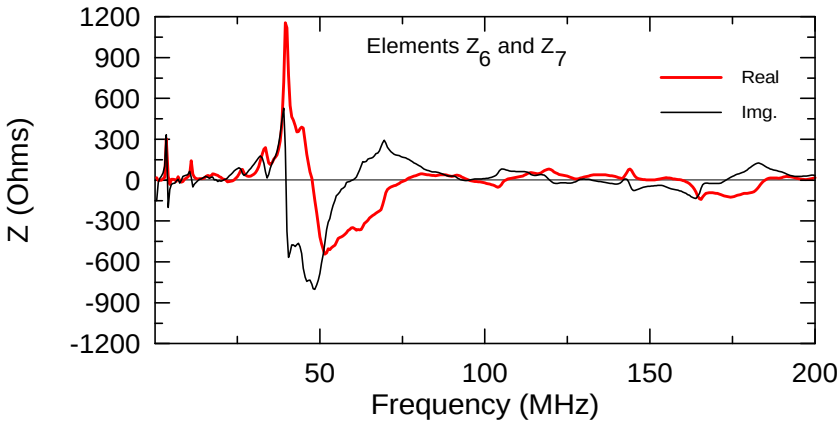

c. Elements Z_6 and Z_7

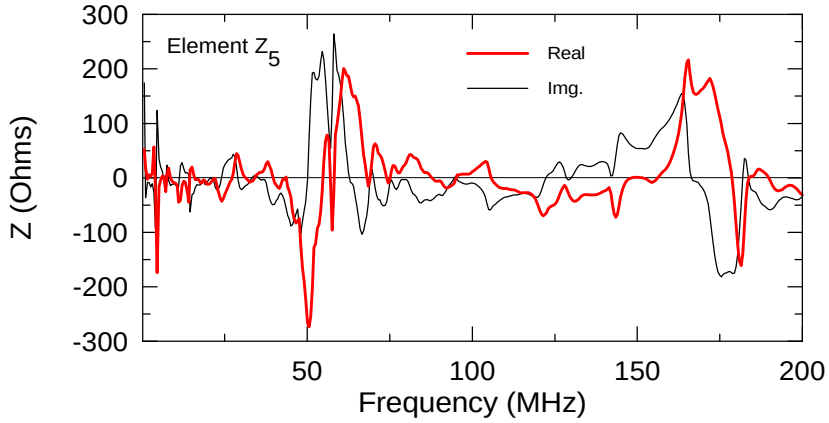

d. Elements Z_5

Figure 10. Plots of the frequency dependence of the equivalent Tee circuit elements for the transformer, as determined from the s-parameter measurements.

In addition to the broadband CW measurements made on this 1.2 kV transformer, a pulse injection test also was conducted. In this test, a 10 Ω pulser with an amplitude of about 15 kV was connected to the two transformer inputs (in common mode), and two 50 Ω loads were placed across each secondary winding. The transformer input port voltages were measured, as well as the load voltages. These voltages were also calculated using the transformer model, and a comparison of the measured and calculated peak values of the responses were made. In addition, the model permits the calculation of the transformer currents, although these latter quantities were not measured.

Table 4 presents a comparison of the measured and calculated peak responses for the 1.2kV-120.240V distribution-class power transformer. Notice that the current transfer ratio (an average of –13.5 dB) compares favorably with the current attenuation measurements made for the Swedish generation facility in Section 3.1, although the transformers are radically different. The voltage attenuation of this transformer (on the order of 25 dB), however, is significantly larger than the values estimated for other transformers. It may be due to the fact that in the pulse measurements, there was no attempt to duplicate the power system connected to the transformer. Only the isolated transformer was measured, and the 10

Ω source and 50 Ω load impedances are not representative of the actual input and output sections of the power system.

Table 4. Comparison of the measured and calculated peak voltage response ratios for the 1.2kV-120/240V distribution transformer.

Response quantity	Measured response (dB)	Calculated response (dB)
V_3/V_1	-25.4	-27.
V_4/V_2	-23.5	-23.3
I_3/I_1	--	-15.2
I_4/I_2	--	-12.0

4. Transformer Failure Tests

Only a limited amount of data on transformer failures to HEMP surges appears to have been recorded. The power community has had considerable experience with lightning-induced transformer failures, but these surges are slower than the HEMP surges, and it is not clear that such lightning data are immediately applicable. One useful HEMP test, which did provide failure data, is described in the next section.

4.1. Distribution transformer vulnerability testing

As part of the Oak Ridge National Laboratory EMP Program, the Westinghouse Electric Corporation performed tests on nineteen standard commercial 7.2 kV – 240/120V, 25 kVA distribution transformers to determine the vulnerability of their insulation to steep-front, short-duration (SFSD) pulses [9].

These transformers were tested, both with and without surge arresters, using the high voltage pulser at Maxwell Laboratories in San Diego, CA, which has been described previously in Section 3.2. For these tests, the system configuration of Figure 11 was used. The open circuit pulser test voltages V_{out} were 400 kV, 500 kV, 800 kV and 1000 kV. These voltages reportedly exhibited a rise time of approximately 60 ns and a fall time of 2000 ns time to half value.

As shown in the figure, the pulser voltage was applied to the transformer being tested through a 400 Ω series resistor to represent the surge impedance of a connected power line. Standard lightning impulse tests for this voltage class of distribution transformer were conducted prior to the SFSD tests to verify the insulation integrity, and were repeated following each SFSD test to ascertain if an insulation failure had occurred in the tested transformer.

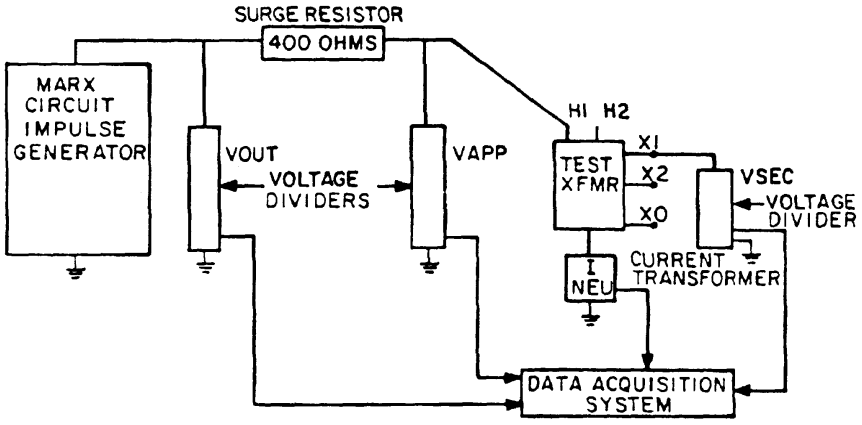

Figure 11. Schematic diagram of the pulser and transformer configuration for the Westinghouse tests of the 7.2 kV, 25 kVA transformers.

As an example of the measured waveforms taken in these transformer tests, Figure 12 plots a typical open circuit voltage waveform across the pulser [10]. Note that this response is denoted as V_{out} in Figure 11. The corresponding measured voltage at the transformer primary terminals (denoted as V_{app} in Figure 11) with and without a surge arrestor is illustrated in Figure 13.

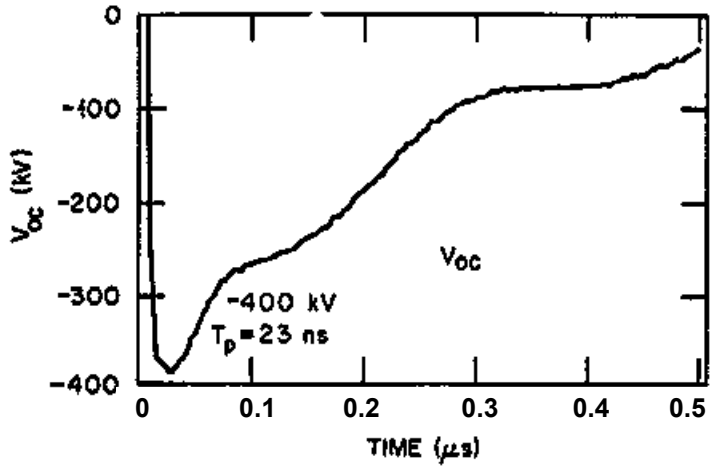

Figure 12. Plot of a typical open circuit pulser voltage for the 7.3 kV, 25 kVA transformer testing (also denoted as V_{out} in Figure 11.)

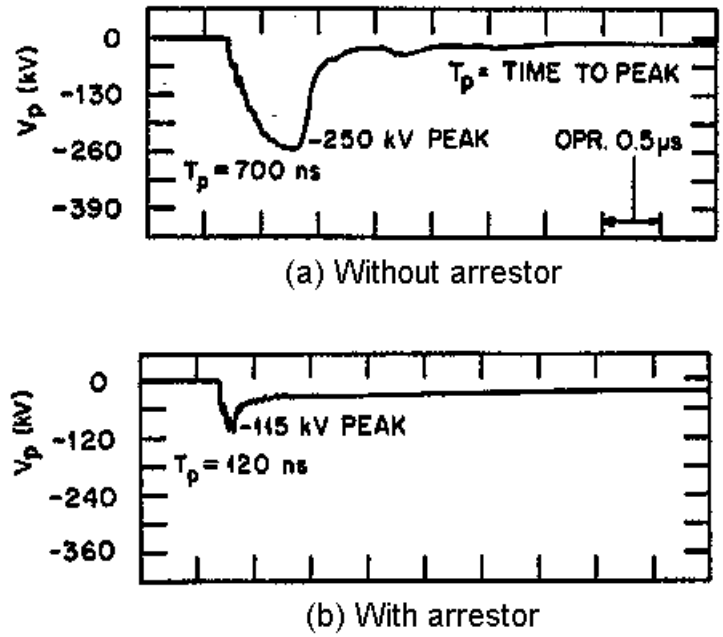

Figure 13. Example of the measured transformer primary voltage (denoted as V_{app} in Figure 11) with and without a surge arrestor on the transformer primary circuit.

Figure 14 presents the measured transformer secondary voltage (denoted as V_{sec} in Figure 11) with a surge arrestor on the transformer primary circuit. From these data we note that there is approximately a peak voltage attenuation of approximately 13.3 dB for this 25 kVA transformer with this loading configuration. This value is consistent with the other transformer tests described in Section 3.

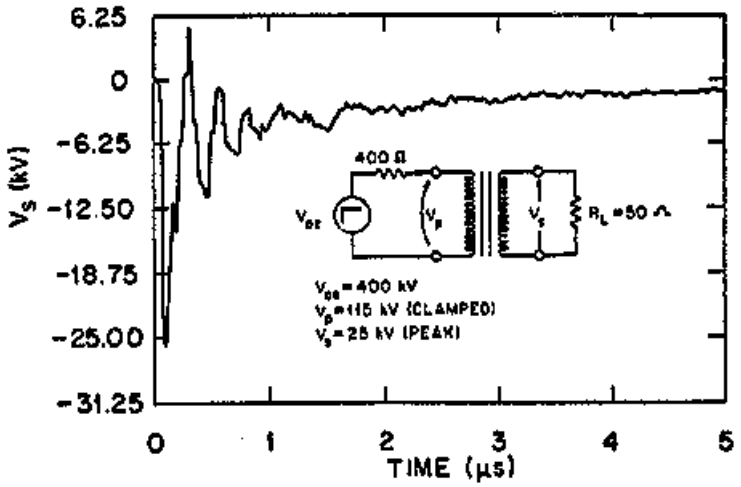

Figure 14. Example of the measured transformer secondary voltage (denoted as V_{sec} in Figure 11) with a surge arrestor on the transformer primary circuit.

4.2. Transformer failure summary

After each pulse on the transformers, an assessment as to whether the transformer had failed was made. Failed transformers were disassembled to evaluate the failure modes. It was determined that no insulation failures occurred on any transformers tested that were protected by surge arresters mounted directly on the transformer housing. An external flashover of the high voltage bushing occurred in some cases when a surge arrester did not protect the transformer, but the bushing flashover was not always sufficient to protect the transformer.

Unprotected transformers failed at voltages around 250 kV to 300 kV peak. The failure mode was usually due to an internal flashover of puncture between the first few turns of an outer layer of the high voltage winding and the low voltage winding, or, sometimes, to an inner layer of the high voltage winding.

The results from this test program are summarized in Table 5, and the conclusions of this study as reported in [9] are as follows:

1. For SFSD surges at 400-kV open circuit levels, unprotected (non-arrester protected) transformers experienced several external flashovers of the surged high voltage bushing. In at least two cases external flashovers of the high voltage bushing resulted in layer-to-layer damage in the high-voltage winding. In other cases, there was no evidence of internal damage although external bushing flashover occurred. Thus, it may be concluded that external flashover of the high voltage bushing of transformers not protected by surge arresters does not always guarantee protection of the transformer. Corona rings eliminated external flashover of the high-voltage bushings but absence of external flashover always resulted in transformer failure.
2. For SFSD surges at the 400-kV level, unprotected transformers, with no external flashover, developed major internal dielectric failures. These failures usually consisted of a puncture from the first few turns of the high-voltage winding to the low-voltage winding and to the wire going to the overload light.
3. For SFSD surges at the 400-kV level, surge arrester-protected transformers experienced no external flashovers of the high voltage bushing and no internal

damage. Surge arresters mounted directly on the transformer protected the transformer from damage in all cases tested.

4. Application of surge arresters, with the surge arrester installed on the transformer tank, provided adequate protection against these surges. No internal damage occurred to any of the units tested where they were protected by surge arresters in this manner.
5. For SFSD surges at 500-kV, 800-kV, and 1000 kV open circuit levels, surge-arrester protected transformers experienced no external flashovers and no internal damage when the surge arresters were mounted on the transformer tank.
6. For SFSD surges at the 800-kV open-circuit level, remotely mounted surge arresters were less effective at protecting transformer than surge arresters mounted on the transformer. Transformer failure was experienced for remote arrestors, compared with no failures experienced at any voltage when the surge arresters were mounted directly on the transformer tank.

Table 5. Summary of Westinghouse 7.2 kV, 25 kVA distribution transformer tests (from reference [9]).

Transformer	Shots #@kV	Crest Voltage* (kV)	Time to Crest (ns)	Surge Arrestor	Notes	Result
ZS2	1@400	264	618	No	(1)	T-T Fail
ZS3	2@400	288	668	No	(2)	HV-LV Fail
ZS4	2@400	280	600	No	(1)	L-L Fail
ZS5	1@400	272	550	No	(2)	HV-LV Fail
ZS6	2@400	290	643	No	(1)	No Damage
ZV1	1@400	296	601	No	(1)	No Damage
ZV2	1@400	304	592	No	(2)	HV-LV Fail
ZV3	2@400	110	100	Yes	(3)	No Damage
ZV4	2@500 2@780	110 116	100 110	Yes Yes	(3) (3)	No Damage No Damage
XV1	1@400	272	500	No	(2)	HV-LV Fail
XV2	2@400	115	110	Yes	(3)	No Damage
ZW1	2@400	292	552	No	(1)	No Damage
ZW2	2@400	16	Oscillatory	No	(4)	No Damage
ZW3	2@780	100	110	Yes	(3)	No Damage
ZW4	2@1000	112	105	Yes	(3)	No Damage
ZD1	2@400	120	550	No	(5)	No Damage
ZD2	2@400	20	Oscillatory	No	(4)	No Damage
ZE1	2@1000	95	100	Yes	(6)	No Damage
ZE2	6@780	95	100	Yes	(6)	No Damage

* Magnitude of the "loaded" voltage waveform across the transformer primary. All waveshapes approximately a 60 ns × 2000 ns double exponential shape. All waveforms negative polarity. BIL of transformer = 95 kV.

Notes

1. External flashover on HV bushing: T-T fail denoted turn-to-turn failure; L-L fail denoted layer-to-layer failure
2. No external flashover; HV-LV fail denotes a high-voltage winding flashover to the low-voltage winding
3. Surge arrestor operation and no external flashover
4. Surge applied to low voltage bushings, no external flashover
5. Surge applied to common mode to both HV bushings, external flashover
6. Surge applied to common mode to both bushings, both arresters operated

The transformer failure measurements summarized in Table 5 can be used to develop a statistical model for describing the failures in these 7.2 kV, 25 kVA distribution transformers.

Using the measured data of Table 5, an estimate of the probability density for the transformer failure can be developed. For an assumed *normal* distribution for the transformer failures given by the expression

$$P_f(x) = \frac{1}{\sqrt{2p}\,s} e^{-\frac{1}{2}\left(\frac{x-m}{s}\right)^2}$$

with $x = V_{app}/V_{BIL}$, a mean value of $m = 2.947$ and a variance of $s^2 = 0.0227$ was determined from the data. In this expression, V_{BIL}, denotes the basic insulation level (BIL) voltage, which is a measure of the robustness of the internal insulation of the transformer. This voltage varies depending on the voltage class of the power system. For the 7.2 kV, 25 kVA transformer used for these tests, the stated BIL was 95 kV, and this value serves as a convenient reference voltage to describe of the electrical stress applied to the transformer.

Figure 15 presents the cumulative probability distribution (CPD) as determined from the above equation, as a function of the normalized applied voltage ratio of V_{app}/V_{BIL}.

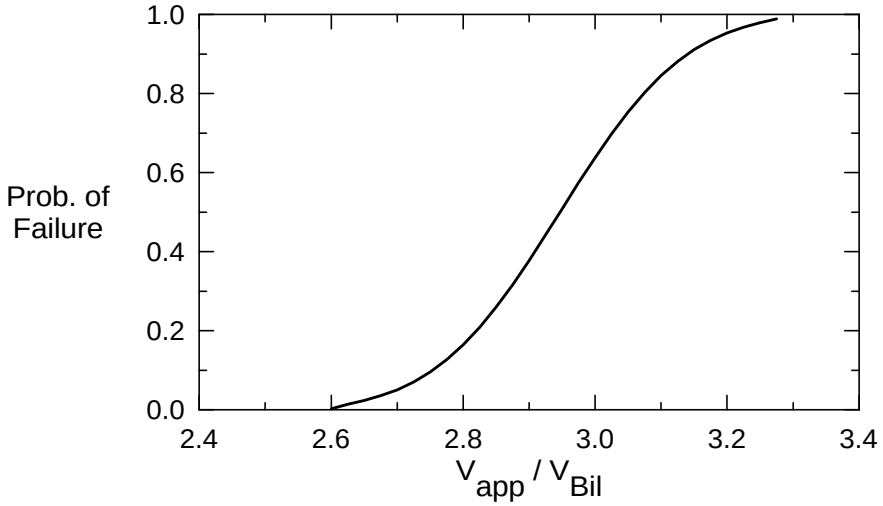

Figure 15. Plot of the probability of failure for the 7.2 kV, 25 kVA power transformer, as a function of the ratio of V_{app}/V_{BIL} for the 60 ns ´ 2000 ns excitation pulse.

5. Summary

Using the previously discussed test data for transformers subjected to HEMP surges, one can develop an understanding of the filtering of the surges, as well as the possible failure of the transformers. Table 6 summarizes the measured HEMP surge attenuation ratios that were collected for the various transformer tests described in this report. With the exception of the test result for the 1.2 kV distribution transformer, all measured attenuation ratios are similar. As mentioned previously, while the 1.2 kV distribution transformer test ultimately served to characterize accurately the transformer by its four-port parameters, it was done in a manner that did not adequately mock-up the actual power system configuration. Consequently, its attenuation characteristics can be considered as anomalous, and they are neglected in estimating a power transformer surge attenuation value.

Table 6. Summary of observed surge attenuation characteristics for various transformer tests.

Transformer Test	Quantity	Attenuation (dB)
25 kVA with filter & surge arrestors	Voltage	14.4
25 kVA silicon and amorphous core	Voltage	12.6 (with protection) 11.2 (without protection)
Swedish pulse injection	Current	14.0
1.2 kV distribution transformer	Voltage	24.0
Westinghouse test of 7.2 kV, 25 kVA transformer	Voltage	13.3

From the measured transformer responses, therefore, we can postulate that an *average* of the various attenuations will provide a suitable surge attenuation model for transformers. Performing an average of the data in Table 6 (on the numerical values of the attenuation, not on the dB values themselves) yields an attenuation figure of about 13 dB.

With regard to the failure of transformers by HEMP pulses, it is unfortunate that only a limited amount of failure data could be found in the literature. However, the data for the 25 kV transformers suggest that the failure occurs with a 50 % probability at an applied voltage of about 2.9 times the rated BIL of the transformer, for a 60 ns × 2000 ns pulse excitation. It is possible that these failure data could be extrapolated to other waveforms or to other transformers having different BILs.

6. References

1. Tesche, F. M., and P. R. Barnes, “The HEMP Response of an Overhead Power Distribution Line”, *IEEE Trans. Power Delivery*, Vol. 4, No. 3, July 1989.
2. Vance, E.F., “Electromagnetic-Pulse Handbook for Electric Power Systems”, *Report DNA 3466F*, Defense Nuclear Agency, Washington DC, February 4, 1975.
3. Karlsson, T., G. Unden and M. Gylmo, “EMP Simulation by Pulse Injection”, *Proceedings of the 6th Symposium and Technical Exhibition on EMC*, Zurich, March 5-7, 1985.
4. Tesche, F. M., and P. R. Barnes, "Extrapolation of Measured Power System Response Data to High-Altitude EMP Excitation," *IEEE Trans. EMC*, Vol. 30, No.3, August 1988.
5. “HEMP Testing of Filter and Transformers”, Maxwell Laboratories final report MLR-3310, prepared for Naval Civil Engineering Laboratory, Port Hueneme, CA, July 28, 1989.
6. “HEMP Testing of Silicon Steel and Amorphous Core Transformers”, Maxwell Laboratories final report MLR-3312, prepared for EH&G, Idaho, Inc., Idaho Falls, ID, May 31, 1989.
7. Tesche, F. M., et. al., **EMC Analysis Methods and Computational Models**, Joun Wiley and Sons, New York, 1997.
8. Pozar, D. M., **Microwave Engineering**, Addison Wesley, New York, 1990.
9. Eichler, C. H, J. R. Legro, and P. R. Barnes, “Experimental Determination of the Effects of Steep Front, Short Duration Surges on 25 kVA Pole Mounted Distribution Transformers”, Paper 88 SM 545-6, presented at the IEEE/PES 1988 Summer Meeting, Portland OR, July 24-29, 1988.
10. Unpublished data from Westinghouse Electric Corp., provided to P. R. Barnes, Oak Ridge National Laboratory, circa 1989.